journal

J. Am. Ceram. Soc., 79 [5] 1163–68 (1996)

Computer Simulation Model for Coupled Grain Growth and Ostwald Ripening—Application to Al_2O_3–ZrO_2 Two-Phase Systems

Long-Qing Chen and Danan Fan

Department of Materials Science and Engineering, The Pennsylvania State University, University Park, Pennsylvania 16802

A kinetic model based on generalized continuum time-dependent Ginzburg–Landau (TDGL) equations is proposed for studying coupled grain growth and Ostwald ripening in multiphase systems. In this model, an arbitrary multiphase microstructure is described by many orientation field variables which represent crystallographic orientations of grains in each phase and by $n - 1$ composition field variables which distinguish the compositional differences among n phases. Microstructural development during simultaneous grain growth and Ostwald ripening is predicted by the temporal evolution of these field variables by numerically solving the TDGL equations. A particular example, Al_2O_3–ZrO_2 particulate composite, was considered. The effects of the volume fraction of ZrO_2 on the microstructural features and their evolution were studied and compared to experimental observations and previous thermodynamic analysis.

I. Introduction

GRAIN growth is a process in which the average grain size of a single-phase polycrystalline material increases with time, driven by the reduction in the total grain boundary energy. The driving force for a given boundary to move is the difference in the chemical potentials of an atom on the opposite sides of the grain boundary, which may be written as

$$\Delta\mu = \sigma_{gb}\Omega(H_1 + H_2) \tag{1}$$

where $\Delta\mu$ is the chemical potential change for an atom going from one side of the grain boundary to another, σ_{gb} is the grain boundary energy, Ω is the atomic volume, and $(H_1 + H_2)$ is the local mean curvature. The velocity of boundary migration is determined by the rate at which atoms jump across the boundary.

$$V = B\Delta\mu \tag{2}$$

where V is the grain boundary migration velocity and B is the boundary mobility. The typical diffusion distance for atoms involved in a grain boundary migration is, therefore, on the order of the boundary width which, for a pure material, is about two or three lattice parameters.

On the other hand, Ostwald ripening usually refers to a process during which large second-phase particles grow while small particles dissolve in a matrix, resulting in a reduction in the total interfacial energy between the precipitates and matrix. The driving force is the difference in the chemical potentials of atoms in large and small second-phase particles, which results in a difference in the compositions of solute atoms in the matrix immediately outside the second-phase particles.

$$\Delta\mu = \sigma_{\alpha\beta}\Omega\left(\frac{1}{r_1} - \frac{1}{r_2}\right) \tag{3}$$

where $\Delta\mu$ is the chemical potential difference of a solute atom in two particles with respective radii of r_1 and r_2, $\sigma_{\alpha\beta}$ is the interfacial energy between the precipitate (α) and matrix (β), and Ω is the atomic volume of a solute atom. In order for a large particle to grow, however, solute atoms outside a small particle have to diffuse through the matrix to regions near the large particle. Therefore, the typical diffusion distance for atoms involved in the Ostwald ripening process is on the order of the separation distance between second-phase particles.

Due to their different characteristics, grain growth and Ostwald ripening were usually treated as two separate processes. For example, essentially all classical mean-field and statistical theories of normal grain growth as well as recent computer simulations considered only pure single-phase systems,[1] whereas theoretical models of Ostwald ripening considered only single crystals and thus avoided the complexity due to grain boundaries.[2]

In many ceramics and metallic alloys of practical application, in particular, in multiphase polycrystalline materials, grain growth and Ostwald ripening may take place simultaneously. Important examples include the ZrO_2–Al_2O_3 two-phase particulate composite in ceramics[3–5] and the two-phase ($\alpha + \beta$) titanium alloys in metallic systems.[6,7] Even in single-phase materials, second-phase precipitates were often observed at grain boundaries, and they may undergo Ostwald ripening during grain growth. In fact, pores may be treated as a second phase during sintering.

There have been numerous theoretical attempts to study the effect of second-phase particles on grain growth kinetics. Most of the theoretical models[7,8] and Q-states Potts model simulations[10–12] considered small and immobile second-phase particles which cannot coarsen. Recently, the thermodynamics of a two-phase microstructure, in which the volume fractions of the two constituent phases are not conserved, have been analyzed by Cahn,[13] and the corresponding kinetics of grain growth and microstructural evolution were studied by Holm *et al.*[14] using the Potts model.

The main purpose of this paper is to propose a new approach for simulating the kinetics of coupled grain growth and Ostwald ripening in systems in which the volume fractions are conserved. It is based on our recent computer simulation model for grain growth in single-phase systems,[15–17] in which the grain boundaries are described in the spirit of the diffuse-interface theory of Cahn and Hilliard.[18] Computer simulations using this model will allow one not only to monitor the detailed microstructural evolution during coupled grain growth and Ostwald ripening but also to obtain information about the average grain size and size distribution of all the phases. As an example, the Al_2O_3–ZrO_2 system was considered. The emphasis will be on the microstructural features predicted from the computer simulation and on their comparison to experimentally observed ones. The unique features of topological changes observed during coupled-grain growth and Ostwald ripening, as compared to single-phase normal grain growth, will be discussed. The

R. Raj—contributing editor

Manuscript No. 193110. Received October 26, 1994; approved November 27, 1995.
Supported by the National Science Foundation under Grant No. DMR 93-11898. The computing time was provided by the Pittsburgh Supercomputing Center under Grant No. DMR 94-0015P.

detailed kinetics of grain growth in Al_2O_3–ZrO_2, such as the time dependence of grain size and size distributions, the topological changes and distributions, and the effect of different diffusion paths (boundary or lattice diffusion), will be reported in a future publication.

II. The Model

(1) Description of the Microstructure of a Two-Phase Solid

The microstructure of a fully dense two-phase solid is schematically shown in Fig. 1, which comprises two phases: α and β, with different compositions, and very often, different crystal structures. There are, in principle, an infinite number of different crystallographic orientations in space for the grains of the two phases, and, roughly speaking, there are three different boundaries: grain boundaries in α, grain boundaries in β, and the interphase boundaries between α and β. These boundaries may be viewed as material regions with certain thicknesses, within which atoms are not in perfect crystal lattice positions. We assumed that across a boundary the composition or crystallographic orientation continuously varies from one grain to another; i.e., we treat grain and interphase boundaries as diffuse interfaces with finite thickness.

Within this diffuse-interface context, we describe an arbitrary two-phase polycrystalline microstructure using a set of continuous field variables,

$$\eta_1^\alpha(r),\eta_2^\alpha(r),\ldots,\eta_p^\alpha(r),\eta_1^\beta(r),\eta_2^\beta(r),\ldots,\eta_q^\beta(r),C(r) \qquad (4)$$

where $\eta_i^\alpha(i = 1,\ldots,p)$ and $\eta_j^\beta(j = 1,\ldots,q)$ are called orientation field variables with each representing grains of a given crystallographic orientation of a given phase. Those variables change continuously in space and assume continuous values ranging from −1.0 to 1.0. For example, a value of 1.0 for $\eta_1^\alpha(r)$, with values for all the other orientation variables 0.0 at r, means that the material at position r belongs to an α grain with the crystallographic orientation labeled as 1. Within the grain boundary region between two α-grains with orientation 1 and 2, $\eta_1^\alpha(r)$ and $\eta_2^\alpha(r)$ will have absolute values intermediate between 0.0 and 1.0. $C(r)$ is the composition field which takes the value of C_α within an α grain and C_β with a β grain. $C(r)$ has intermediate values between C_α and C_β across an α/β interphase boundary.

Following Cahn and Hilliard,[18] the total free energy of a two-phase system, F, can be written as

$$F = \int\left[f_0(C(r);\eta_1^\alpha(r),\eta_2^\alpha(r),\ldots,\eta_p^\alpha(r);\eta_1^\beta(r),\eta_2^\beta(r),\ldots,\eta_q^\beta(r)) + \frac{\kappa_C}{2}[\nabla C(r)]^2 + \sum_{i=1}^{p}\frac{\kappa_i^\alpha}{2}[\nabla\eta_i^\alpha(r)]^2 + \sum_{i=1}^{q}\frac{\kappa_i^\beta}{2}[\nabla\eta_i^\beta(r)]^2\right]d^3r \qquad (5)$$

where f_0 is the local free energy density, κ_C, κ_i^α, and κ_i^β are the gradient energy coefficients for the composition field and orientation fields, and p and q represent the number of orientation field variables for α and β. The cross-gradient energy terms have been ignored for simplicity.

The energy of a planar grain boundary, σ_{gb}^α, between an α-grain of orientation i and another α-grain of orientation j may be calculated as follows:

$$\sigma_{gb}^\alpha = \int_{-\infty}^{+\infty}\left[\Delta f(\eta_i^\alpha,\eta_j^\alpha,C) + \frac{\kappa_C}{2}\left(\frac{dC}{dx}\right)^2 + \frac{\kappa_i^\alpha}{2}\left(\frac{d\eta_i^\alpha}{dx}\right)^2 + \frac{\kappa_j^\alpha}{2}\left(\frac{d\eta_j^\alpha}{dx}\right)^2\right]dx \qquad (6)$$

in which

$$\Delta f(\eta_i^\alpha,\eta_j^\alpha,C) = f_0(\eta_i^\alpha,\eta_j^\alpha,C) - f_0(\eta_{i,e}^\alpha,\eta_{j,e}^\alpha,C_\alpha) - (C - C_\alpha)\left(\frac{\partial f_0}{\partial C}\right)_{\eta_{i,e}^\alpha,\eta_{j,e}^\alpha,C_\alpha} \qquad (7)$$

where $f_0(\eta_{i,e}^\alpha,\eta_{j,e}^\alpha,C_\alpha)$ represents the free energy density minimized with respect to η_i^α and η_j^α at the equilibrium composition of α, C_α. The grain boundary energy for β can be calculated similarly. The definition of grain boundary energy (6) includes the composition gradient term and automatically takes into account the effect of solute segregation to grain boundaries.

The interphase boundary energy between an α-grain with orientation i and a β-grain with orientation j is given by

$$\sigma_{int}^{\alpha\beta} = \int_{-\infty}^{+\infty}\left[\Delta f(\eta_i^\alpha,\eta_j^\beta,C) + \frac{\kappa_C}{2}\left(\frac{dC}{dx}\right)^2 + \frac{\kappa_i^\alpha}{2}\left(\frac{d\eta_i^\alpha}{dx}\right)^2 + \frac{\kappa_j^\beta}{2}\left(\frac{d\eta_j^\beta}{dx}\right)^2\right]dx \qquad (8)$$

where

$$\Delta f(\eta_i^\alpha,\eta_j^\beta,C) = f_0(\eta_i^\alpha,\eta_j^\beta,C) - f_0(\eta_{i,e}^\alpha,\eta_{j,e}^\beta,C_\alpha) - (C - C_\alpha)\left(\frac{\partial f_0}{\partial C}\right)_{\eta_{i,e}^\alpha,\eta_{j,e}^\beta,C_\alpha} \qquad (9a)$$

or

$$\Delta f(\eta_i^\alpha,\eta_j^\beta,C) = f_0(\eta_i^\alpha,\eta_j^\beta,C) - f_0(\eta_{i,e}^\alpha,\eta_{j,e}^\beta,C_\beta) - (C - C_\beta)\left(\frac{\partial f_0}{\partial C}\right)_{\eta_{i,e}^\alpha,\eta_{j,e}^\beta,C_\beta} \qquad (9b)$$

(2) Kinetic Equations

By defining orientation and composition field variables, the kinetics of coupled grain growth can be described by their spatial and temporal evolution. In the present model, the evolution kinetics of these field variables are described by the time-dependent Ginzburg–Landau (TDGL) equations, which are the continuum Allen–Cahn[19] and Cahn–Hilliard[18] equations.

$$\frac{d\eta_i^\alpha(r,t)}{dt} = -L_i^\alpha\frac{\delta F}{\delta\eta_i^\alpha(r,t)} \qquad i = 1, 2, \ldots, p \qquad (10a)$$

$$\frac{d\eta_i^\beta(r,t)}{dt} = -L_i^\beta\frac{\delta F}{\delta\eta_i^\beta(r,t)} \qquad i = 1, 2, \ldots, q \qquad (10b)$$

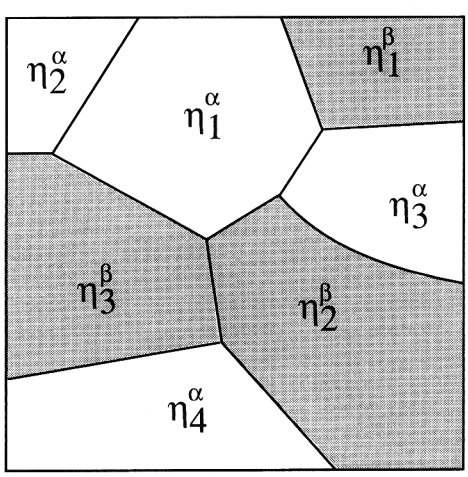

Fig. 1. Schematic description of a two-phase microstructure. $\eta_i^\alpha(i = 1,\ldots,p)$ and $\eta_i^\beta(j = 1,\ldots,q)$ are orientation field variables with each representing grains of a given crystallographic orientation of a given phase (denoted as α or β).

$$\frac{dC(r,t)}{dt} = \nabla\left\{L_C\nabla\left[\frac{\delta F}{\delta C(r,t)}\right]\right\} \quad (10c)$$

where L_i^α, L_i^β, and L_C are kinetic coefficients related to grain boundary mobilities and atomic diffusion coefficients, which may be functions of local orientation and composition field variables, t is time, and F is the total free energy. It may be noticed that the cross terms in the right-hand side of (10) have been neglected. The difference between kinetic equations for orientation fields and concentration fields comes from the fact that concentration is a conserved field which satisfies local and global mass conservation or conservation of phase–volume fractions in a system, whereas an orientation field is nonconserved, since the volume fraction of grains of a given orientation is not conserved.

Substituting the free energy functional F in (5) into the kinetic equation (10) gives

$$\frac{d\eta_i^\alpha}{dt} = -L_i^\alpha\left[\frac{\partial f_0}{\partial \eta_i^\alpha} - \kappa_i^\alpha\nabla^2\eta_i^\alpha\right] \qquad i = 1, 2, \ldots, p \quad (11a)$$

$$\frac{d\eta_i^\beta}{dt} = -L_i^\beta\left[\frac{\partial f_0}{\partial \eta_i^\beta} - \kappa_i^\beta\nabla^2\eta_i^\beta\right] \qquad i = 1, 2, \ldots, q \quad (11b)$$

$$\frac{dC}{dt} = \nabla L_C\nabla\left[\frac{\partial f_0}{\partial_C} - \kappa_C\nabla^2 C\right] \quad (11c)$$

(3) Construction of the Local Free Energy Density Function of a Homogeneous Phase

In order to solve the kinetic equations and thus simulate the coupled grain growth and Ostwald ripening for a given system, the thermodynamics of the system need to be specified. For this purpose, we need to construct the free energy functional, f_0. f_0 should have the following characteristics: (a) If the values of all the orientation field variables are zero, it describes the dependence of the free energy of the liquid phase on composition. (b) The free energy density as a function of composition in a given α-phase grain is obtained by minimizing f_0 with respect to the orientation field variable corresponding to that grain under the condition that all other orientation field variables are zero. (c) The free energy density as a function of composition of a given β-phase grain may be obtained in a similar way. Therefore, all the phenomenological parameters in the free energy model, in principle, may be fixed using the information about the free energies of the liquid, solid α-phase and solid β-phase.

Another main requirement for f_0 is that it has p degenerate minima with equal depth located at $(\eta_1^\alpha, \eta_2^\alpha, \ldots, \eta_p^\alpha) = (1,0,\ldots,0)$, $(0,1,\ldots,0)$, …, $(0,0,\ldots,1)$ in p-dimension orientation space at the equilibrium concentration C_α, and has q degenerate minima located at $(\eta_1^\beta, \eta_2^\beta, \ldots, \eta_q^\beta) = (1,0,\ldots,0)$, $(0,1,\ldots,0)$, …, $(0,0,\ldots,1)$ at C_β. This requirement ensures that each point in space can belong to only one crystallographic orientation of a given phase.

(4) Determination of Other Thermodynamic and Kinetic Parameters

Once the free energy functional, f_0, is obtained, the gradient energy coefficients can be fitted to the grain boundary energies of α and β as well as the α/β boundary energy by numerically solving Eqs. (6) and (8). The kinetic coefficients, L_i^α, L_i^β, and L_C, in principle, can be fitted to grain boundary mobility and atomic diffusion data.

III. Application to Al_2O_3–ZrO_2 and Discussions

For the purpose of illustrating the application of the present model, a particular system, Al_2O_3–ZrO_2, in which the microstructural evolution has been extensively investigated experimentally, is considered. Unfortunately, however, the thermodynamics of this system are not well characterized. Therefore, since we do not have the free energy information about the Al_2O_3–ZrO_2 two-phase system, we construct the following free energy functional:

$$\begin{aligned} f_0(\eta_1^\alpha(r), \eta_2^\alpha(r), \ldots, \eta_p^\alpha(r); \eta_1^\beta(r), \eta_2^\beta(r), \ldots, \eta_q^\beta(r); C(r)) = \\ -\frac{A}{2}[C(r) - C_m]^2 + \frac{B}{4}[C(r) - C_m]^4 \\ + \frac{D_\alpha}{4}[C(r) - C_\alpha]^4 + \frac{D_\beta}{4}[C(r) - C_\beta]^4 \\ + \sum_{i=1}^{p}\left\{-\frac{\gamma_\alpha}{2}[C(r) - C_\beta]^2[\eta_i^\alpha(r)]^2 + \frac{\delta_\alpha}{4}[\eta_i^\alpha(r)]^4\right\} \\ + \sum_{i=1}^{q}\left\{-\frac{\gamma_\beta}{2}[C(r) - C_\alpha]^2[\eta_i^\beta(r)]^2 + \frac{\delta_\beta}{4}[\eta_i^\beta(r)]^4\right\} \\ + \frac{\varepsilon}{2}\sum_\alpha\sum_\beta\sum_{i=1}^{p}\sum_{j=1}^{q}[\eta_i^\alpha(r)]^2[\eta_j^\beta(r)]^2 \end{aligned} \quad (12)$$

where C_α and C_β are the equilibrium compositions of α and β phases or solubilities, $C_m = (C_\alpha + C_\beta)/2$, A, B, D_α, D_β, γ_α, γ_β, δ_α, δ_β, and ε are phenomenological parameters.

It should be emphasized that since we are not interested in phase transformations between α and β, the exact form of the free energy density function may not be very important in modeling microstructural evolution in a two-phase solid. The reason is that the driving force for grain growth is the total grain and interphase boundary energy. Other important parameters are the diffusion coefficients and boundary mobilities. In other words, we assume that the values of the grain and interphase boundary energies together with the kinetic coefficients completely control the kinetics of microstructural evolution, irrespective of the form of the free energy density function.

It should also be pointed out that the absolute values of the grain and interphase boundary energies may not be very important, whereas their ratios actually play a key role in determining the microstructural features of a two-phase solid, and it is the ratios that can be experimentally measured. In the Al_2O_3–ZrO_2 system, it was reported[20] that the ratio of grain boundary energy in Al_2O_3 (denoted as α phase) to the interphase boundary energy between Al_2O_3 and ZrO_2 is $R_\alpha = \sigma_{alu}^\alpha/\sigma_{int}^{\alpha\beta} = 1.4$, and the ratio of grain boundary energy in ZrO_2 (denoted as β phase) to the interphase boundary energy is: $R_\beta = \sigma_{zir}^\beta/\sigma_{int}^{\alpha\beta} = 0.97$. Because of the anisotropy of grain boundary energies and the interphase boundary energy, there are actually distributions of R_α and R_β instead of a single value. However, in this paper, for simplicity, we ignored the distributions. To adjust the gradient coefficients (κ_C, κ_i^α, and κ_i^β) and phenomenological parameters in the free energy density function to produce these experimentally determined ratios, the equilibrium profiles of the orientation fields and the composition field across a flat boundary (either grain boundary or an interphase boundary) were first obtained, and then substituted to Eq. (6) or (8) to calculate the grain or interphase boundary energy. We also assumed that the solubilities are 1% of one phase in another ($C_\alpha = 0.01$, $C_\beta = 0.99$). It is found that parameters $A = 2.0$, $B = 9.88$, $D_\alpha = D_\beta = 1.52$, $\gamma_\alpha = \gamma_\beta = 1.23$, $\delta_\alpha = \delta_\beta = 1.0$, $\varepsilon = 1.0$, $\varepsilon = 7.0$, $\kappa_C = 1.5$, $\kappa_i^\alpha = 2.5$, and $\kappa_i^\alpha = 2.0$ give the experimentally determined energetic ratios for the Al_2O_3–ZrO_2 system. The grain boundary energies and the interphase boundary energy were assumed isotropic. Furthermore, we also assume isotropic grain boundary mobility, and the chemical diffusion coefficient is assumed to be the same in the two phases. Since we can always normalize the length and time scales of kinetic equations with the diffusion coefficient and boundary mobilities, we simply choose $L_\eta^\alpha = L_\eta^\beta = 1.0$ and $L_C = 0.5$.

To solve the set of kinetic equations (11), the Laplacian was discretized by the following equation:

$$\nabla^2\phi = \frac{1}{(\Delta x)^2}\left[\frac{1}{2}\sum_j(\phi_j - \phi_i) + \frac{1}{4}\sum_{j'}(\sigma_{j'} - \phi_i)\right] \quad (13)$$

where ϕ is a field variable, Δx is the grid size, j represents the

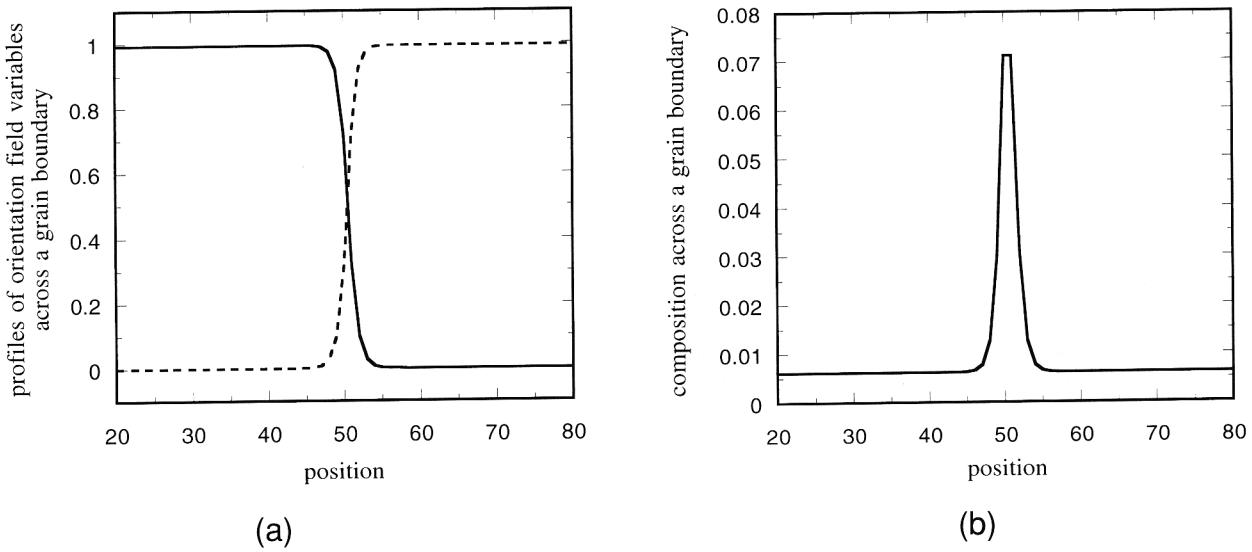

Fig. 2. (a) Profiles of orientation field variables across a grain boundary separating two grains with orientations labeled as 1 and 2 in the α phase. Solid line—the profile of orientation field variable 1 (η_1^α); dotted line—the profile of orientation field variable 2 (η_2^α). (b) The composition profile across a grain boundary showing significant segregation in a single phase with overall average composition 0.01.

set of first nearest neighbors of i, and j' is the set of second nearest neighbors of i. The kinetic equations were then solved using the simple explicit Euler technique.

All the results were obtained by using $\Delta x = 2.0$ and Δt (the time step for integration) $= 0.25$. For simplicity, the computer simulations were carried out in two dimensions with 256×256 points and with periodic boundary conditions applied along both directions. The total number of orientation field variables $(p + q)$ is 30.

To initiate a computer simulation, one may either input a predefined initial two-phase microstructure or generate one by assigning small random values to all the orientation field variables and the overall average composition to the composition variable at all grid points, which simulates a liquid at a high temperature. In this paper, the initial microstructures were generated from fine grain structures produced by a normal grain growth simulation, and then by randomly assigning all the grains to either α or β according to the desired volume fractions. We assumed that the microstructural evolution takes place isothermally.

To visualize the microstructures produced from the computer simulation, the following function is defined:

$$\psi(r) = 0.75\left(\sum_{i=1}^{p} [\eta_i^\alpha(r)]^2\right) + \sum_{i=1}^{q} [\eta_i^\beta(r)]^2 \qquad (14)$$

For example, $\psi(r)$ may be displayed by using gray-levels with low and high values represented by dark and bright, respectively. With this definition, the values of $\psi(r)$ within a β grain are close to 1.0 and within an α grain close to 0.75, while those at the boundaries are close to zero or significantly less than 1.0. Therefore, the bright regions will be β grains (ZrO_2), gray regions are α grains (Al_2O_3), and the dark lines are grain or interphase boundaries.

The equilibrium profiles of orientation fields and composition field across a flat grain boundary in α are shown in Figs. 2(a) and (b). It can be seen that, across a grain boundary, the values of an orientation field continuously change from one grain to another. The composition profile (Fig. 2(b)) shows significant segregation at the grain boundaries. The composition profile across an interphase boundary between α and β is shown in Fig. 3.

The microstructural evolutions in systems with 10%, 20%, and 40% of ZrO_2 are shown in Figs. 4, 5, and 6, respectively. The simulated microstructures appear to have a striking resemblance to those observed experimentally.[4,5,20] More importantly, the main features of coupled grain growth and Ostwald ripening, as observed experimentally and discussed in,[5,20] are predicted by the computer simulations. At low volume fraction of ZrO_2, the ZrO_2 grains are mainly located at trijunctions and grain boundaries of Al_2O_3, and coarsening of ZrO_2 grains is controlled by the Ostwald ripening process; i.e., relatively large ZrO_2 grains grow at the expense of smaller ones by long-range diffusion. The motion of Al_2O_3 grain boundaries is essentially pinned by the ZrO_2 grains, and the grain size of Al_2O_3 grains is more or less fixed by the locations and distributions of ZrO_2 particles. Once a ZrO_2 particle disappears at a given trijunction or grain boundary, the coarsening of Al_2O_3 grains and the readjustment of the grain topology around that junction takes place quite rapidly. The number of Al_2O_3 grain boundaries pinned is determined by the number of ZrO_2 particles and the volume fraction of ZrO_2. At low volume fraction of ZrO_2, the number of ZrO_2 particles available for pinning is small; as a result, the rate of grain growth is greater than in systems with relatively high volume fractions (compare Figs. 4, 5, and 6). At high volume fraction of ZrO_2 (Fig. 6), grains of

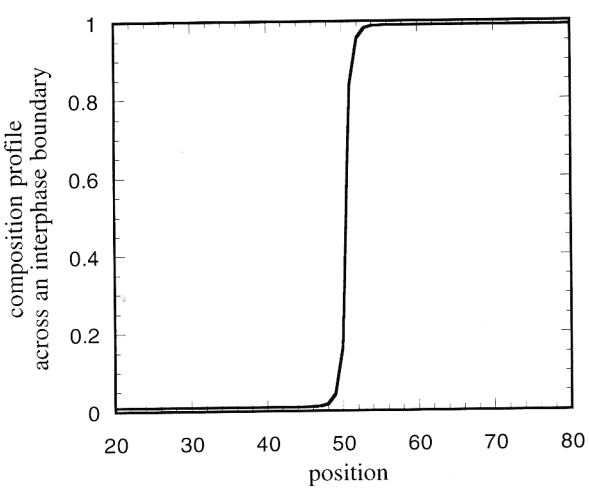

Fig. 3. Composition profile across an interphase boundary between α and β.

the two phases are more or less interconnected and mutually pinned.

Although the thermodynamic analysis by Cahn[13] was made on a system in which the volume fraction of the second phase is nonconserved, Alexander[20] was able to predict, using the same analysis, some of the topological features in Al_2O_3–ZrO_2, in which the volume fractions are conserved. In Al_2O_3–ZrO_2, the grain boundary energy in Al_2O_3 is much higher than that of ZrO_2 ($R_\alpha = 1.4$, $R_\beta = 0.97$). Therefore, the thermodynamic equilibrium angles at the trijunctions formed by two α grains and a β grain (ααβ) are different from those formed by one α grain and two β grains (αββ). At a trijunction αββ, the equilibrium angle (ϕ_α) in the α phase is given by $2 \cos(\phi_\alpha/2) = R_\beta$ and that in the β phase at a trijunction ααβ is given by $2 \cos(\phi_\beta/2) = R_\alpha$.[13] Using the values of R_α and R_β for Al_2O_3–ZrO_2, we have $\phi_\alpha = 121.98°$ and $\phi_\beta = 91.19°$. As a result, an isolated Al_2O_3 (α) grain (surrounded by ZrO_2 grains) will have convex boundaries if the number of grain edges is equal to or less than 6. On the other hand, an isolated ZrO_2 (β) grain is concave until the number of grain edges is less than 4. It is reminded that in single-phase grain growth with isotropic grain boundary energies, grains with less than 6 edges tend to be convex and shrink.

From Figs. 4 and 5, it can be seen that most of the isolated ZrO_2 grains with 4 and more edges have concave boundaries, which is consistent with the thermodynamic analysis.[20] However, some isolated ZrO_2 grains in Figs. 4 and 5 have mixed concave and convex boundaries, even though they have more than 4 edges. The direction of curvatures can change during a microstructural evolution. This can be clearly seen from the evolution of the grain labeled A in Fig. 4. This grain initially had 6 concave edges. It then transformed to a 5-sided and then 4-sided grain with mixed concave and convex boundaries. There are two possible reasons for the departure from the thermodynamic prediction. First, the balance of surface tension is determined by the tangents of those boundaries meeting at a trijunction; hence, the balance can be accomplished either by a

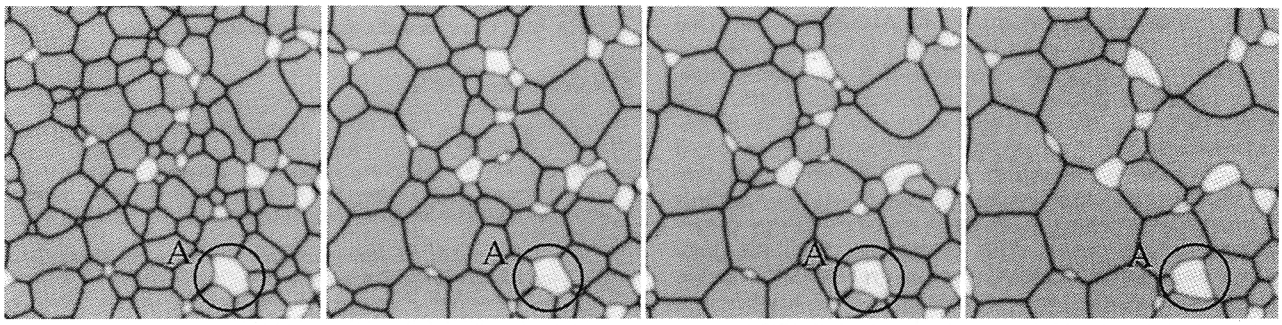

Fig. 4. Temporal microstructural evolution in Al_2O_3–10% ZrO_2 system. (a) Time step = 6000; (b) time step = 12 000; (c) time step = 21 000; (d) time step = 30 000.

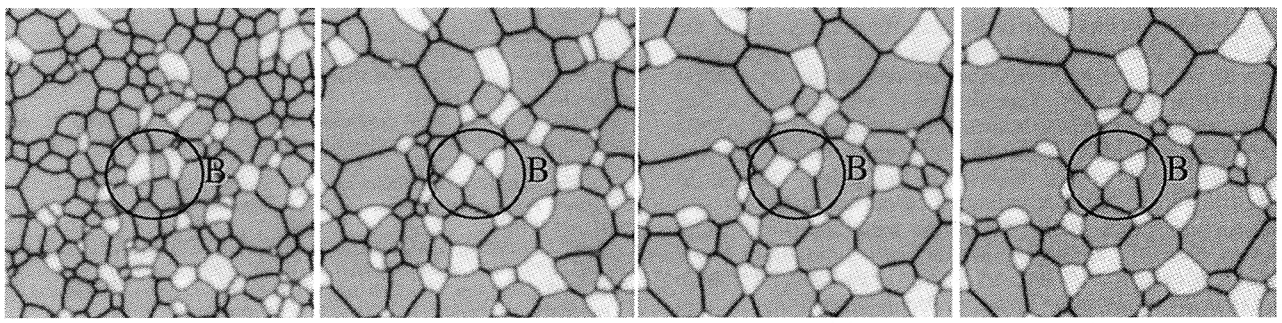

Fig. 5. Temporal microstructural evolution in Al_2O_3–20% ZrO_2 system. (a) Time step = 3000; (b) time step = 12 000; (c) time step = 21 000; (d) time step = 30 000.

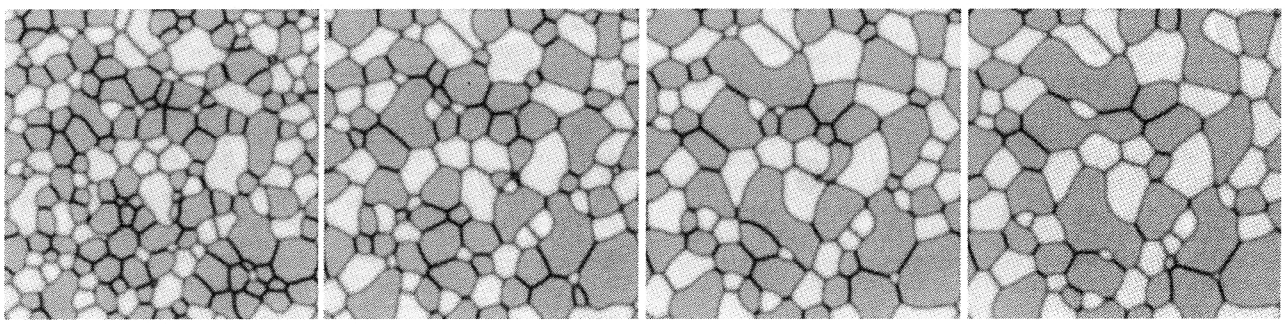

Fig. 6. Temporal microstructural evolution in Al_2O_3–40% ZrO_2 system. (a) Time step = 3000; (b) time step = 12 000; (c) time step = 21 000; (d) time step = 30 000.

concave and a convex boundary, or two concave boundaries, as long as the tangents of these two boundaries provide the same angle at the trijunction. Second, the topological change of a β grain is due to the coarsening of neighboring α grains, which results in the shape change and the mass redistribution of the β grain to accommodate the space-filling requirement. The mass redistribution requires the diffusion of atoms along the interphase boundaries or through volume diffusion, which is driven by the chemical potential difference at different boundaries with different curvatures around the β grain. Hence, it is the local shape adjustment and mass redistribution that lead to the formation of mixed concave and convex boundaries. It should be noted that the area of this β grain changes very slowly, because the coarsening of this grain is governed by the long-distance diffusion or Ostwald ripening, while the topological transformation and mass redistribution occur relatively rapidly, which is controlled by the local boundary diffusion.

During microstructural evolution, there is a tendency to eliminate Al_2O_3 grain boundaries, because the energy of a Al_2O_3 grain boundary is much higher than that of a ZrO_2 grain boundary and that of the interphase boundary energy between Al_2O_3 and ZrO_2, which has been discussed by Alexander *et al.*[5] One way to eliminate Al_2O_3 grain boundaries is by coarsening or grain growth of Al_2O_3 grains. However, if Al_2O_3 grain boundaries are pinned by ZrO_2 grains, the second mechanism, grain boundary switching, occurs. This can be seen from the evolution of grains in Fig. 5 labeled as B. In this region, an initial Al_2O_3 grain boundary is replaced by a ZrO_2 grain boundary during the microstructural evolution. The driven force for this grain boundary switching is the grain boundary energy difference between two phases. This is different from the grain boundary switching in single-phase grain growth with isotropic grain boundary energies, in which the grain boundary between two smaller grains would disappear. However, in this system, the grain boundary between two larger Al_2O_3 grains disappeared because of its higher energy. As a result, as the volume fraction of ZrO_2 increases, the Al_2O_3 grains become increasingly separated by ZrO_2 grains. For example, at 40% of ZrO_2, most Al_2O_3 grains are isolated by ZrO_2 grains.

Finally, it should be mentioned that one of the popular existing computer simulation techniques for grain growth is the Monte Carlo simulation technique based on the Q-state Potts model, in which the grain orientations are labeled by integer numbers from 1 to Q.[21,22] Therefore, it is worthwhile pointing out some of the differences between the present model and the Q-state Potts model. First of all, both grain boundaries and interphase boundaries are diffuse in the present model, as opposed to Monte Carlo simulations of normal grain growth, which assumed that grain boundaries were sharp with zero thickness. Secondly, unlike the Monte Carlo simulations based on the Q-state Potts model, in which grain and interphase boundaries are made up of kinks, all boundaries in the present model are smooth. Third, in the present model the anisotropy resulting from the discretization of the kinetic equations can be minimized by using enough grid points to resolve the interfacial regions, whereas in Monte Carlo simulations, interactions beyond the nearest neighbors can be introduced to reduce the effect of lattice anisotropy.[22] Finally, in the present model, the atomic diffusion process is automatically described by the Cahn–Hilliard nonlinear diffusion equation, while in Monte Carlo simulations, it is rather tricky, although it is not impossible, to describe the long-range diffusion process such as Ostwald ripening.[23]

With the addition of a heat conduction equation, the present model can also be employed to simulate the microstructural evolution during solidification and subsequent grain growth and Ostwald ripening. As a matter of fact, the phase-field model widely employed in solidification modeling uses one phase-field variable (called orientation-field variable in this paper) and the composition-field variable to describe the dendritic growth morphology.[24]

IV. Conclusions

A computer simulation approach based on the continuum Ginzburg–Landau model with many orientation fields, and a composition field is developed for investigating coupled grain growth and Ostwald ripening in two-phase systems. Its application to the ZrO_2–Al_2O_3 particulate composite shows that it can reproduce essentially all the microstructural features observed experimentally. Although the general feature of a two-phase microstructure can be predicted from a thermodynamic analysis based on the grain boundary energy to interphase boundary energy ratios, the details of the topology, the number of sides, and curvatures of the boundaries of a second-phase grain depends also on the local environment, the size, and spatial distribution of neighboring matrix grains. While grain boundary switching in a single-phase grain growth with isotropic grain boundary energies results in the disappearance of the grain boundary between two smaller grains, in Al_2O_3–ZrO_2 grain switching leads to elimination of Al_2O_3 grain boundaries as a result of their high energy as compared to ZrO_2 grain boundaries.

Acknowledgments: The authors are grateful to Dr. C. A. Handwerker for bringing to our attention the experimental studies of two-phase grain growth in Al_2O_3–ZrO_2, to Dr. K. B. Alexander for providing us a copy of her short-course notes given at the 1995 ACerS Annual Meeting, and to Dr. J. W. Cahn and Dr. W. C. Carter for useful discussions at many occasions.

References

[1]H. V. Atkinson, "Overview No. 65—Theory of Normal Grain Growth in Pure Single Phase Systems," *Acta Metall.*, **36**, 469 (1988), and references therein.

[2]P. W. Voorhees, "Ostwald Ripening of Two-Phase Mixtures," *Annu. Rev. Mater. Sci.*, **22**, 197–215 (1992), and references therein.

[3]J. D. French, M. P. Harmer, H. M. Chan, and G. A. Miller, "Coarsening-Resistant Dual-Phase Interpenetrating Microstructures," *J. Am. Ceram. Soc.*, **73**, 2508 (1990).

[4]F. F. Lange and M. M. Hirlinger, "Grain Growth in Two-Phase Ceramics: Al_2O_3 Inclusions in ZrO_2," *J. Am. Ceram. Soc.*, **70**, 827 (1987).

[5]K. B. Alexander, P. F. Becher, S. B. Waters, and A. Bleier, "Grain Growth Kinetics in Alumina–Zirconia (CeZTA) Composites," *J. Am. Ceram. Soc.*, **77**, 939 (1994), and references therein.

[6]S. Ankem and H. Margolin, "Grain Growth Relationships in Two-Phase Titanium Alloys"; p. 1705 in Proceedings of International Conference on Titanium (Munich, FRG, 1984); Vol. 3. Deutsche Gesellsschaft fur Metallkunde, FRG, 1985.

[7]G. Grewal and S. Ankem, "Modeling Matrix Grain Growth in the Presence of Growing Second Phase Particles in Two Phase Alloys," *Acta Metall. Mater.*, **38**, 1607 (1990).

[8]C. S. Smith, "Grains, Phases, and Interfaces: An Interpretation of Microstructure," *Trans, AIME*, **175**, 15 (1948).

[9]M. Hillert, "Inhibition of Grain Growth by Second-Phase Particles," *Acta Metall.*, **36**, 3177 (1988).

[10]D. J. Srolovitz, M. P. Anderson, G. S. Grest, and P. S. Sahni, "Computer Simulation of Grain Growth—III. Influence of a Particle Dispersion," *Acta Metall.*, **32**, 1429 (1984).

[11]R. D. Doherty, D. J. Srolovitz, A. D. Rollett, and M. P. Anderson, "On the Volume Fraction Dependence of Particle Limited Grain Growth," *Scr. Metall.*, **21**, 675 (1987).

[12]G. N. Hassold, E. A. Holm, and D. J. Srolovitz, "Effects of Particle Size on Inhibited Grain Growth," *Scr. Metall.*, **24**, 101 (1990).

[13]J. W. Cahn, "Stability, Microstructural Evolution, Grain Growth, and Coarsening in a Two-Dimensional Two-Phase Microstructure," *Acta Metall.*, **39**, 2189 (1991).

[14]E. A. Holm, D. J. Srolovitz, and J. W. Cahn, "Microstructural Evolution in Two-Dimensional Two-Phase Polycrystals," *Acta Metall. Mater.*, **41**, 1119 (1993).

[15]L. Q. Chen and W. Yang, "Computer Simulation of the Domain Dynamics of a Quenched System with a Large Number of Nonconserved Order Parameters: Grain Growth Kinetics," *Phys. Rev. B*, **50**, 15752 (1994).

[16]L. Q. Chen, "A Novel Computer Simulation Technique for Modeling Grain Growth," *Scr. Metall. Mater.*, **32**, 115 (1995).

[17]D. Fan and L. Q. Chen, "Computer Simulation of Grain Growth Using a Continuum Field Model," submitted to *Acta Metall. Mater.*, 1995.

[18]J. W. Cahn and J. E. Hilliard, "Free Energy of a Nonuniform System. I. Interfacial Free Energy," *J. Chem. Phys.*, **28**, 258 (1958).

[19]S. M. Allen and J. W. Cahn, "A Microscopic Theory for Antiphase Domain Boundary Motion and Its Application to Antiphase Domain Coarsening," *Acta Metall.*, **27**, 1085 (1979).

[20]K. B. Alexander, Short course on "Sintering of Ceramics" at the American Ceramic Society Annual Meeting, Cincinnati, OH, April 1995.

[21]D. J. Srolovitz, M. P. Anderson, G. S. Grest, and P. S. Sahni, "Grain Growth in Two Dimensions," *Scr. Metall.*, **17**, 241 (1983).

[22]M. P. Anderson, D. J. Srolovitz, G. S. Grest, and P. S. Sahni, "Computer Simulation of Grain Growth—I. Kinetics," *Acta Metall.*, **32**, 783 (1984).

[23]V. Tikare, "Numerical Simulation of Grain Growth in Liquid Phase Sintered Materials"; Ph.D. Thesis. Case Western Reserve University, Cleveland, OH, 1994.

[24]A. Wheeler, W. Boettinger, and G. McFadden, "Phase Field Model for Isothermal Phase Transitions in Binary Alloys," *Phys. Rev. A*, **45**, 7424 (1992), and references therein. □